Azimuthal organisation of turbulent structures in underexpanded impinging round jets

Romain Gojon, Christophe Bogey

Azimuthal organisation of turbulent structures in underexpanded impinging round jets

Romain Gojon[1,2,*] and Christophe Bogey[1,†]

1. Laboratoire de Mécanique des Fluides et d'Acoustique

UMR CNRS 5506, Ecole Centrale de Lyon

69134 Ecully, France

2. Department of Mechanics, Royal Institute of Technology (KTH)

Linné FLOW Centre

Stockholm, Sweden

The azimuthal organisation of the turbulent structures in underexpanded round jets impinging on a flat plate have been investigated using compressible large eddy simulation. The jet shear-layer region, as well as the region of the wall jets created on the plate after the impact are considered. The jets are characterized by a Nozzle Pressure Ratio of 4.03, a fully expanded Mach number of 1.56, and a Reynolds number of 6×10^4. The distance between the nozzle and the plate varies from $4.16r_0$ to $9.32r_0$. The jets generate acoustic tones due to a feedback mechanism. In this paper, the near pressure and density fields of the jets are analysed using Fast Fourier Transform on the nozzle exit plane, the plate, and an azimuthal plane. The amplitude and the phase fields on these sections at the tone frequencies are represented. Similar organisations of the turbulent structures are found in the jet shear layers and the wall jets. Thus, axisymmetric and helical arrangements of the structures in the shear layers lead to concentric and spiral distributions of the structures on the plate, respectively. In particular, for one of the jets, a spiral shape and concentric rings, associated with two tone frequencies generated simultaneously, are observed on the flat plate in the pressure and density phase fields. Moreover, the convection velocity of the turbulent structures on the plate is evaluated from the phase fields. Several diameters away from the jet axis, the velocities found for the present jets compare well with those found experimentally in the phase-averaged distributions of fluctuating pressure for impinging ideally expanded jets using fast-response Pressure-Sensitive Paint. Near the jet axis, given that the present jets are underexpanded, differences are observed, due to the presence of shock cell structures in the jets. Finally, the convection velocity of the turbulent structures on the wall are estimated from cross-correlations of radial velocity. The values obtained compare well with those determined from the phase fields.

I. Introduction

Very intense tones have been observed experimentally by Powell[1] and Wagner[2], among others, in the acoustic field of high subsonic and supersonic jets impinging on a flat plate. Powell[1] suggested that such tones are generated by an aeroacoustic feedback mechanism between the turbulent structures propagating downstream from the nozzle to the plate and the acoustic waves propagating upstream from the plate to the nozzle.

For subsonic impinging round jets, the tone frequencies can be predicted by the model proposed by Ho & Nosseir[3] and Nosseir & Ho[4]. Round supersonic jets impinging on a flat plate normally have been investigated experimentally by Henderson & Powell[5], Krothapalli *et al.*[6] and Henderson *et al.*[7] In some cases, a feedback mechanism is observed as in subsonic jets. This is very often the case when the jet is ideally expanded, but this

*PhD, now PostDoc at KTH Mechanics, gojon@kth.se

†CNRS Research Scientist, AIAA Senior Member & Associate Fellow, christophe.bogey@ec-lyon.fr.

happens only for some nozzle-to-plate distances when the jet is imperfectly expanded. Henderson & Powell[5] suggested that, in the latter case, the feedback loop establishes only when a Mach disk forms just upstream from the plate. Recirculation zones were also observed between this Mach disk and the flat plate for some nozzle-to-plate distances by Krothapalli *et al.*[6]. More recently, for underexpanded impinging jets, Risbord & Soria[8] explored the instability modes of the jets using ultra-high-speed Schlieren and shadowgraphy techniques. Axial and helical modes were visualised and the Mach disk located just upstream from the plate was found to oscillate. For similar jets, Buchmann *et al.*[9] pointed out the periodic formation of large-scale structures in the jet shear layers using a high spatial resolution Schlieren imaging. The complete feedback mechanism was visible, namely large-scale structures in the shear layers propagating downstream from the nozzle to the plate and acoustic waves propagating upstream from the plate to the nozzle. Mitchell *et al.*[10] studied the periodic oscillation of the shear layer of underexpanded impinging jets using time-resolved Schlieren image sequences. Finally, Davis *et al.*[11] studied the wall pressure oscillations in ideally expanded impinging jets using a fast-response Pressure-Sensitive Paint on the plate. They identified tone frequencies associated with axisymmetrical and helical oscillation modes of the jets thanks to phase-conditioned Schlieren images. For such modes, they presented the phase-averaged distributions of the fluctuating pressure on the flat plate. The turbulent structures organized axisymmetrically or helically in the jet shear layers were shown to persist after the impact, as they propagate radially in the wall jets, even several diameters away from the jet axis.

In the present study, the azimuthal organisation of turbulent structures in the jet shear-layers and on the flat plate, in the wall jet created after the impact, are studied from data provided by large eddy simulations. The jets are defined by a Nozzle Pressure Ratio of 4.03, a fully expanded Mach number of 1.56, an exit Mach number of 1, and a Reynolds number of 6×10^4. Their aerodynamics and acoustic properties have been analysed previously in detail in Gojon *et al.*[12] The near pressure and density fields of the jets are explored in the present paper using Fast Fourier Transform. In particular, the spatial organisation and the convection velocity of the turbulent structures located in the wall jet created on the plate after the impact are examined. The results are compared with the experimental phase-averaged distributions of the fluctuating pressure of Davis *et al.*[11] for ideally expanded supersonic impinging round jets. For the present underexpanded jets, the presence of shock-cell structures is expected to affect the radial propagation of the structures on the plate. The paper is organised as follows. The numerical methods and the jet properties are presented in section II. An analysis of the turbulent structures in the jet shear-layers and in the wall jets is performed in section III by plotting the amplitude and phase fields of the pressure and density fields at the tone frequencies. Concluding remarks are finally given in section IV.

II. Parameters

II.A. Numerical parameters

In the LES, the unsteady compressible Navier-Stokes equations are solved using cylindrical coordinates (r, θ, z) with an explicit six-stage Runge-Kutta algorithm for time integration, and low-dissipation and low-dispersion explicit eleven-point finite differences for spatial derivation[13,14]. At the end of each time step, a high-order filtering is applied to the flow variables in order to remove grid-to-grid oscillations and to dissipate subgrid-scale turbulent energy[15,16]. The radiation conditions of Tam & Dong[17] are implemented at the boundaries of the computational domain, in combination with a sponge zone at the outflow boundaries combining grid stretching and Laplacian filtering to damp turbulent fluctuations before they reach the boundaries. Adiabatic conditions are imposed at the nozzle walls and at the flat plate. Finally, a shock-capturing filtering is applied in order to avoid Gibbs oscillations near shocks[18]. The axis singularity is treated with the method proposed by Mohseni & Colonius[19]. A reduction of the effective resolution near the origin of the polar coordinates is also implemented[20]. Finally, a forcing[21] is added in the boundary layer in the nozzle in order to generate velocity fluctuations at the nozzle exit.

The simulations are carried out using an OpenMP-based in-house solver, and a total of $180,000$ iterations are performed in each case after the transient period. The simulation time is thus equal to $1000 r_0/u_j$. The cylindrical meshes contain between 171 and 217 million points, as reported in Table 1. They have been designed in order to allow acoustic waves with Strouhal numbers up to $St = fD_j/u_j = 6.4$ to be well propagated.

	n_r	n_θ	n_z	number of points
JetL4	500	512	668	171×10^6
JetL5	500	512	764	195×10^6
JetL7	500	512	780	200×10^6
JetL9	500	512	847	217×10^6

Table 1. Mesh parameters: number of points n_r, n_θ and n_z in the radial, azimuthal and axial direction, and total number of points.

II.B. Jets properties

In this section, the main jet properties are provided. More informations can be found in Gojon *et al.*[12] The jets originate from a pipe nozzle of radius r_0, whose lip is $0.1r_0$ thick. The nozzle-to-plate distances L are respectively equal to $4.16r_0$, $5.6r_0$, $7.3r_0$ and $9.32r_0$, as shown in table 2. The jets are thus referred to as JetL4, JetL5, JetL7 and JetL9. They have an ideally expanded Mach number of $\mathcal{M}_j = u_j/a_j = 1.56$, where u_j and a_j are the exit velocity and the speed of sound in the ideally expanded equivalent jet. Their Reynolds number is $Re_j = u_j D_j/\nu = 6 \times 10^4$, where D_j is the nozzle diameter of the ideally expanded equivalent jet and ν is the kinematic molecular viscosity. The exit Mach number is $\mathcal{M}_e = u_e/a_e = 1$, where u_e and a_e are the exit velocity and the speed of sound in the jet. At the nozzle exit, a Blasius mean velocity profile is imposed with a boundary-layer thickness of $0.15r_0$. The ejection conditions of the jets and the nozzle-to-plate distances are similar to those in the experimental study of Henderson *et al.*[7]

	$\mathcal{M}_j$	Re_j	L
JetL4	1.56	6×10^4	$4.16r_0$
JetL5	1.56	6×10^4	$5.6r_0$
JetL7	1.56	6×10^4	$7.3r_0$
JetL9	1.56	6×10^4	$9.32r_0$

Table 2. Jet parameters: ideally expanded Mach number $\mathcal{M}_j$, Reynolds number Re_j, and nozzle-to-plate distance L.

III. Results

III.A. Snapshots

In order to illustrate the flow fields of the present impinging jets, isosurfaces of density obtained for JetL5 and JetL7 are displayed in figure 1. Shock-cell structures can be seen in the two jets between the nozzle exit and the flat plate. The jet mixing layers and the wall jets developing on the flat plate in the radial direction are well visible. Moreover, both large-scale structures and small-scale vortical structures appear in the mixing layers, in agreement with the Reynolds number Re_j of 6×10^4. The pressure fields in the plane $\theta = 0$ are also represented in figure 1 in order to show the near acoustic field of the jets. The acoustic waves seem to come mainly from the region of jet impact on the flat plate.

III.B. Tone frequencies

The sound pressure levels obtained in the vicinity of the nozzle at $r = 2r_0$ and $z = 0$ are plotted in figure 2 as functions of the Strouhal number $St = fD_j/u_j$. They reveal several tone frequencies. The Strouhal numbers of the tones whose levels are 5 dB higher than the broadband noise are reported in table 3. As detailed in Gojon *et al.*[12], these tones are generated by an aeroacoustic feedback mechanism occurring between the nozzle and the plate, consisting of two steps. First, in the jet shear layers, a turbulent structure is convected in the downstream direction from the nozzle exit to the flat plate. The structure impinges on the plate, and generates an acoustic wave propagating upstream. This wave is reflected back by the nozzle lip, which excites the shear layer, and leads to the formation of a new turbulent structure. The time period of this loop can thus be determined from the convection speed of the shear-layer structures, the speed of the upstream-propagating acoustic waves and the nozzle-to-plate distance. Ho & Nosseir[3] proposed, for instance:

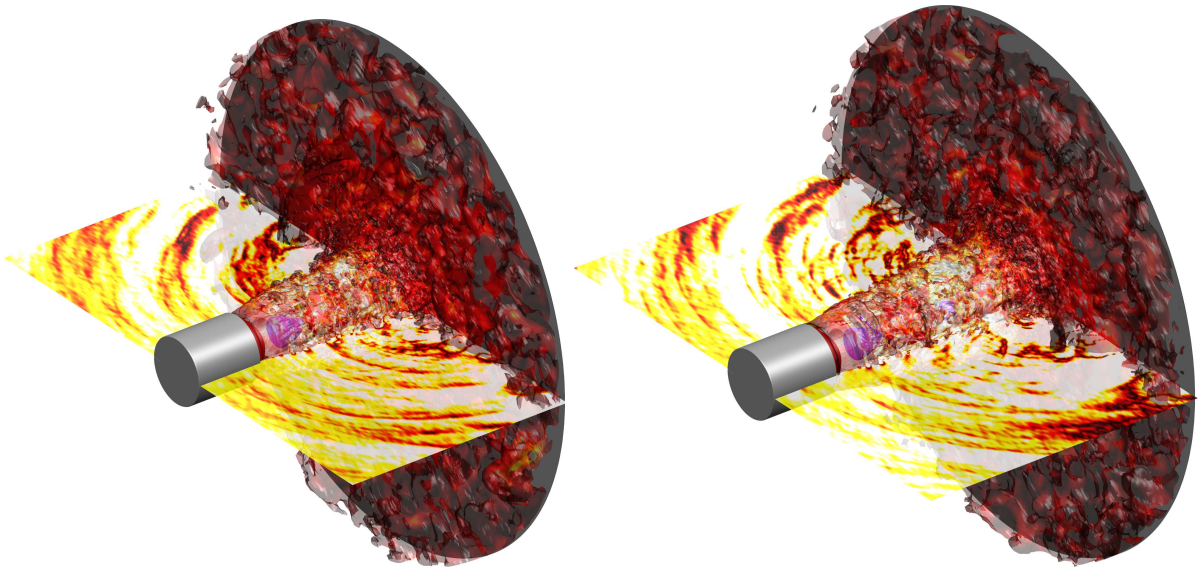

Figure 1. Isosurfaces of density for (a) JetL5 and (b) JetL7. The blue and red isosurfaces are obtained for the values of 0.8 and 2.5 kg.m^{-3}, respectively. The isosurfaces of 1.25 kg.m^{-3} are also represented, colored by the Mach number. The pressure field in the plane $\theta = 0$ is shown. The nozzle and the plate are in grey.

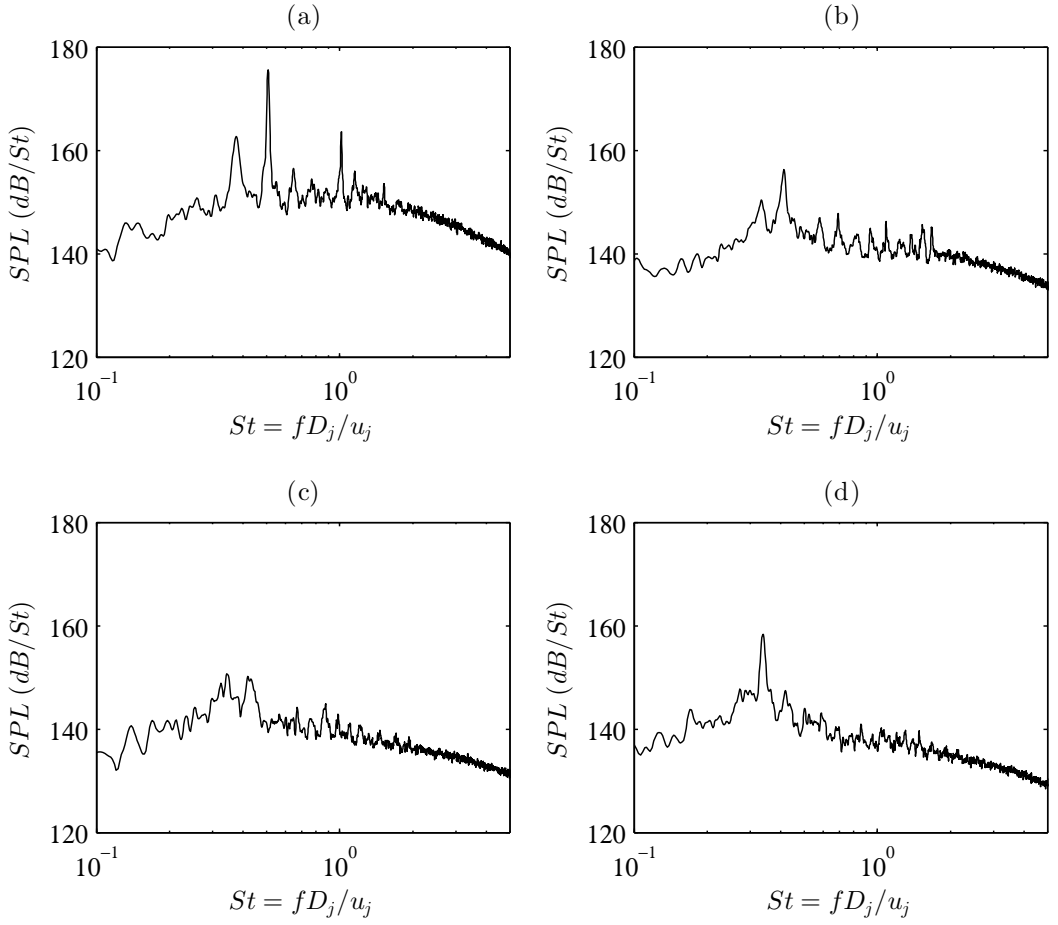

Figure 2. Sound pressure levels at $r = 2r_0$ and $z = 0$ as functions of the Strouhal number for (a) JetL4, (b) JetL5, (c) JetL7 and (d) JetL9.

$$\frac{N}{f} = \frac{L}{< u_c >} + \frac{L}{a_0} \tag{1}$$

where $< u_c >$ is the mean convection velocity of the turbulent structures in the shear layers between the nozzle and the plate, a_0 is the speed of sound in the ambient medium, and N is the mode number indicating the number of times the feedback mechanism occurs during the fundamental period.

	St_1	St_2	St_3
JetL4	0.375	**0.505**	1.01
JetL5	0.335	**0.415**	-
JetL7	**0.345**	0.42	-
JetL9	0.27	**0.34**	0.42

Table 3. Strouhal numbers emerging in the pressure spectra of figure 2. The Strouhal numbers of the dominant tones are in bold.

A very good agreement has been found between the tone frequencies of the present simulated jet, those found in the experimental study of Henderson *et al.*[7], and the frequencies predicted by the relation (1). More details can be found in Gojon *et al.*[12].

III.C. Properties of the near pressure and density fields

In the LES, pressure has been recorded every 50^{th} time step in the planes $z = 0$, $z = L$ and $\theta = 0$. Moreover, density has also been stored every 50^{th} time step in the plane $z = L$. For each plane, the results are arranged in $M \times N$ matrices:

$$P_{all} = \begin{bmatrix} P_1^1 & P_1^2 & . & P_1^N \\ P_2^1 & P_2^2 & . & P_2^N \\ . & . & . & . \\ P_M^1 & P_M^2 & . & P_M^N \end{bmatrix} \tag{2}$$

where N is the number of samplings, and M is the total number of points in the plane. The pressure or density field obtained at a given time is thus provided by one column of the corresponding matrix. A Fast Fourier Transform is applied to each row of the matrices P_{all}. In this way, for a given frequency, the amplitude fields and the phase fields can be displayed. Informations on the oscillation modes of the jet are given by the phase field, and informations on the sound sources are provided by the amplitude and phase fields.

For JetL4, the properties obtained at the two main tone frequencies at $St_1 = 0.375$ and $St_2 = 0.505$ are examined in figures 3 and 4, respectively. For $St_1 = 0.375$, the amplitude and phase fields of the fluctuating pressure at $z = 0$ are given in figures 3(a,e). The amplitude field do not exhibit a clear pattern. On the contrary, the phase field shows two opposite regions out of phase near the jet axis followed by a spiral shape of isophase surfaces. This indicates an helical organisation of the acoustic waves. In the plane $\theta = 0$, in the phase field in figure 3(f), a 180-degree phase shift is visible with respect to the jet axis, suggesting a sinuous or helical oscillation mode of the jet. More precisely, using a Fourier decomposition of the fluctuating pressure on 32 sensors regularly spaced in the azimuthal direction at $z = 0$ and $r = 2r_0$, the mode is found to be helical. Therefore, the feedback mechanism is organised helically at the frequency $St_1 = 0.375$. The amplitude and phase fields of the fluctuating pressure obtained on the plate, at $z = 4.16r_0$ are reported in figures 3(c,g). The amplitude field exhibits a region of high intensity for $r < 2.6r_0$, in the region located inside the jet, under the Mach disk and the annular oblique shock. The phase field, in figure 3(g), shows a spiral shape which extends over the entire domain. At $z = 4.16r_0$, the amplitude and phase fields of the fluctuating density on the plate are presented in figures 3(d,h). They exhibit the same behaviour as that of the pressure fluctuations. The turbulent structures organized helically in the jet shear layers at the tone frequency $St_1 = 0.375$ impinge on the plate and this organisation seems to persist as they propagate radially on the plate.

For $St_2 = 0.505$, the amplitude and phase fields of the fluctuating pressure and fluctuating density are represented in figure 4. The amplitude and phase fields of the fluctuating pressure obtained on the plane $z = 0$ are given in figures 4(a,e). The acoustic waves appear to be organized in a axisymmetric manner.

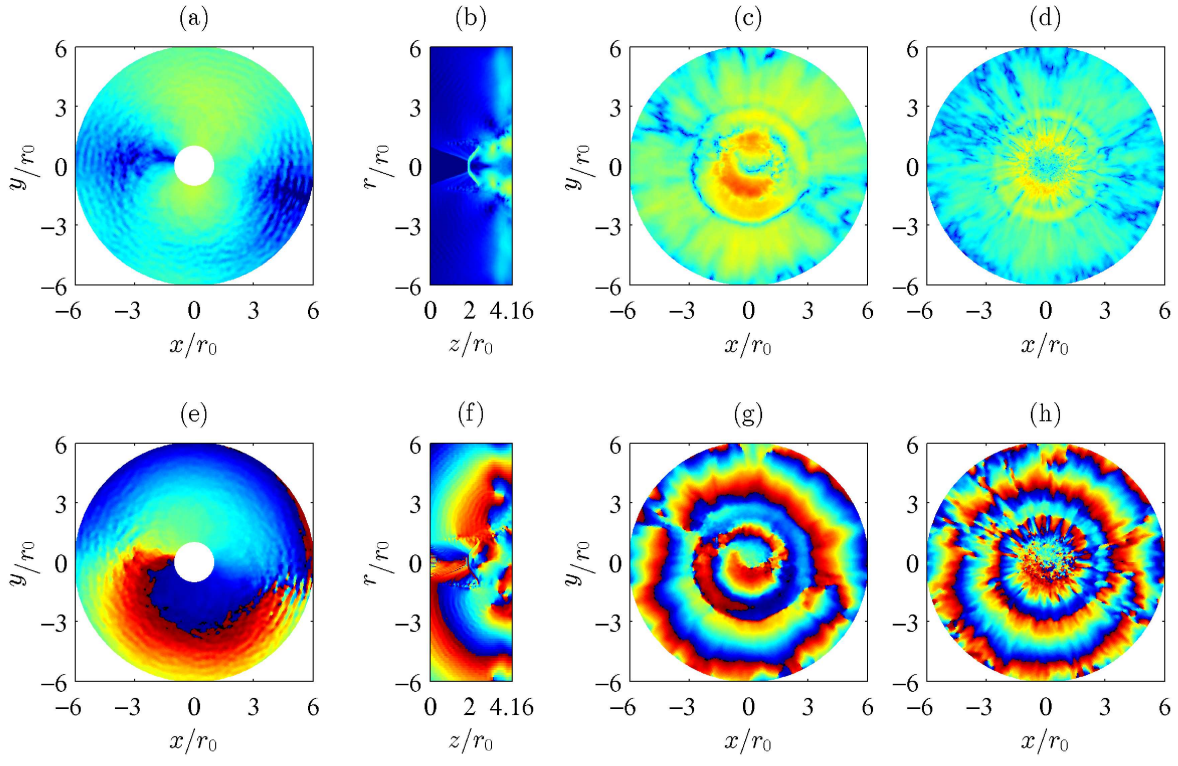

Figure 3. Amplitude (top) and phase (bottom) fields obtained for JetL4 at the tone frequency $St_1 = 0.375$; from pressure (a,e) at $z = 0$, (b,f) at $\theta = 0$ and (c,g) at $z = L$; from density (d,h) at $z = L$.

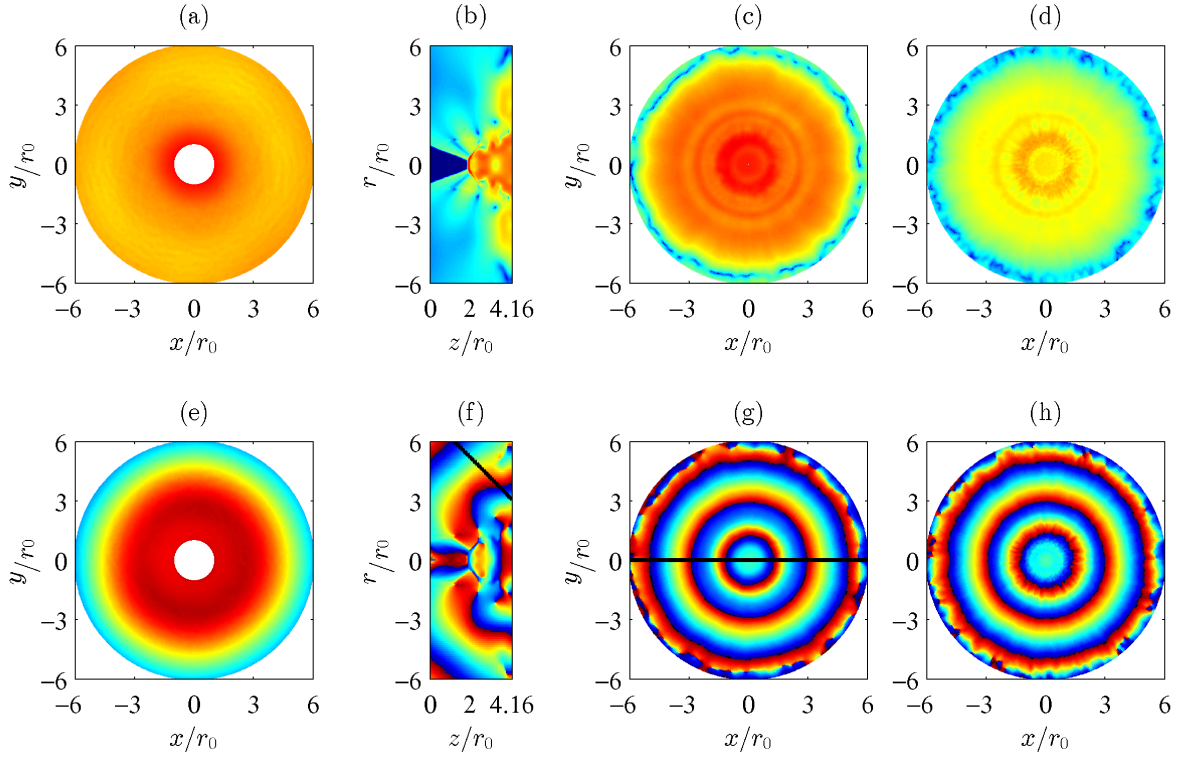

Figure 4. Amplitude (top) and phase (bottom) fields obtained for JetL4 at the dominant tone frequency $St_2 = 0.505$; from pressure (a,e) at $z = 0$, (b,f) at $\theta = 0$ and (c,g) at $z = L$; from density (d,h) at $z = L$.

The amplitude field in the plane $\theta = 0$ of figure 4(b) reveals a cell structure between the nozzle and the plate, containing three cells. This structure has been described in Gojon *et al.*[22]. It is due to the generation of an hydrodynamic-acoustic standing wave by the aeroacoustic feedback mechanism. The number of cells correspond to the mode number of the feedback mechanism in the model of Ho & Nosseir[3]. The phase field, in figure 4(b), exhibits a symmetric organisation with respect to the jet axis, corresponding to an axisymmetric oscillation mode of the jet. Thus, the feedback mechanism is organised axisymmetrically at the frequency $St_2 = 0.505$. In figures 4(g) and 4(h), in the phase fields of the fluctuating pressure and of the fluctuating density on the plate, concentric rings are observed. These rings may be associated with the radial propagation, on the plate, of the coherent structures organised axisymmetrically in the jet shear layers at $St_2 = 0.505$.

In order to confirm the two hypotheses above, phase profiles are represented in figure 5. The first profile considered is the phase profile obtained in the $\theta = 0$ plane, along the black line visible in the phase field of figure 4(f). It is represented in figure 5(a) as a function of the distance l_{impact} from the point located on the wall at $z = 3r_0$. This point was chosen as it corresponds to the location of the source of the acoustic component radiating in the far field, see in Gojon *et al.*[12] The maxima in the phase profile in figure 5(a) are located at $l_{impact} = 1.0r_0$, $4.25r_0$ and $7.6r_0$, giving wavelengths of $3.25r_0$ and $3.35r_0$. The corresponding phase speeds are 327 m.s^{-1} and 338 m.s^{-1}, respectively. They correspond to the ambient sound speed, as expected for acoustic waves. In figure 5(b), the phase profile obtained in the $z = L$ plane along the black line shown in the phase field of figure 4(g) is plotted as a function of the radial coordinate. The wavelength of the concentric rings visible in figures 4(g,h) can thus be measured. The wavelength between the first and the second maxima is $1.75r_0$ and the wavelength between the second and the third maxima is $2.15r_0$. The corresponding phase speeds are equal to $0.40u_j$ and $0.49u_j$, respectively. Given those values, the oscillations obtained at the wall cannot be acoustic waves, but are associated with the radial convection of turbulent structures in the wall jet.

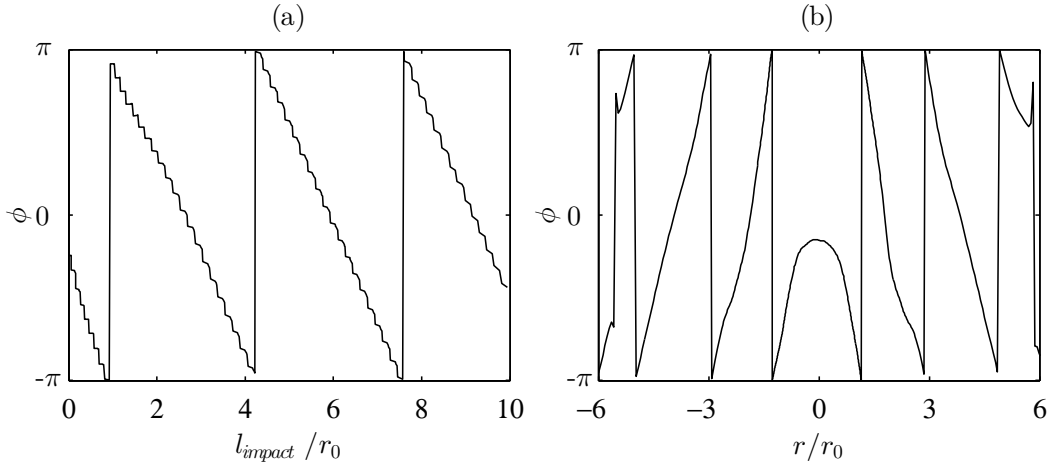

Figure 5. Profiles obtained for JetL4 at $St_2 = 0.505$, (a) in the plane $\theta = 0$ along the black line represented in the phase field of figure 4(f), and (b) in the plane $z = L$ along the black line represented in the phase field of figure 4(g).

For JetL5, the amplitude and phase fields obtained for the two main tone frequencies at $St_1 = 0.335$ and $St_2 = 0.415$ are showed in figures 6 and 7, respectively. Given the pattern of the phase fields at $z = 0$ and $\theta = 0$ in figures 6(e,f) and 7(e,f), these two tones appear to be associated with helical oscillation modes. Moreover, in the phase fields of figures 6(g,h) calculated on the plate for $St_1 = 0.335$ and in figures 7(g,h) for $St_1 = 0.415$, spiral shapes are visible over the entire domain. As for the tone frequency $St_1 = 0.375$ of JetL4, these shapes are due to the radial propagation on the plate of the turbulent structures organized helically in the jet shear layers.

For JetL7, the amplitude and phase fields obtained for the main tone frequency at $St_1 = 0.345$ are given in figure 8. It can be seen from the phase fields in the planes $z = 0$ and $\theta = 0$ in figures 8(e,f) that this tone is linked to an helical jet oscillation mode. The results on the plane $z = L$ show spurious noise because the amplitude of the tone is low compared to the level of tones reported for JetL4 and JetL5 in figure 2. Nevertheless, a spiral shape can be seen in the two phase fields in figures 8(g,h), especially in the phase field of the density field. This shape results from the radial propagation on the plate of the turbulent structures

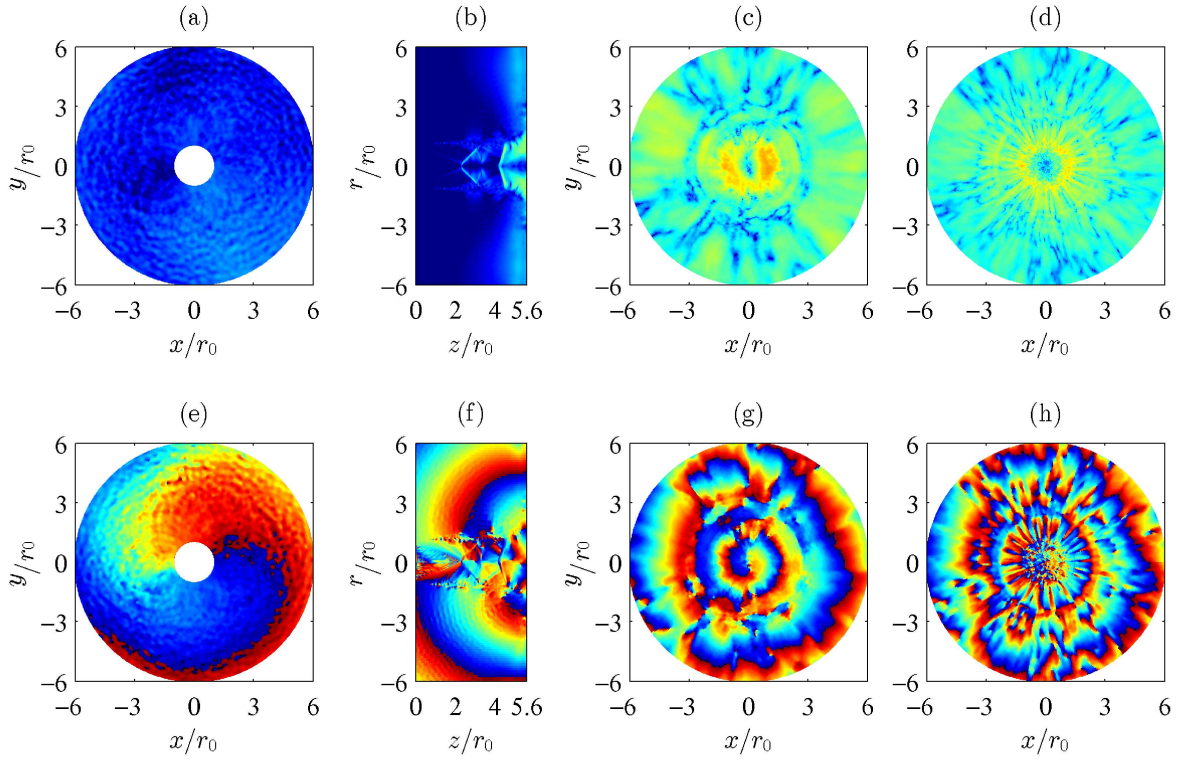

Figure 6. Amplitude (top) and phase (bottom) fields obtained for JetL5 at the tone frequency $St_1 = 0.335$; from pressure (a,e) at $z = 0$, (b,f) at $\theta = 0$ and (c,g) at $z = L$; from density (d,h) at $z = L$.

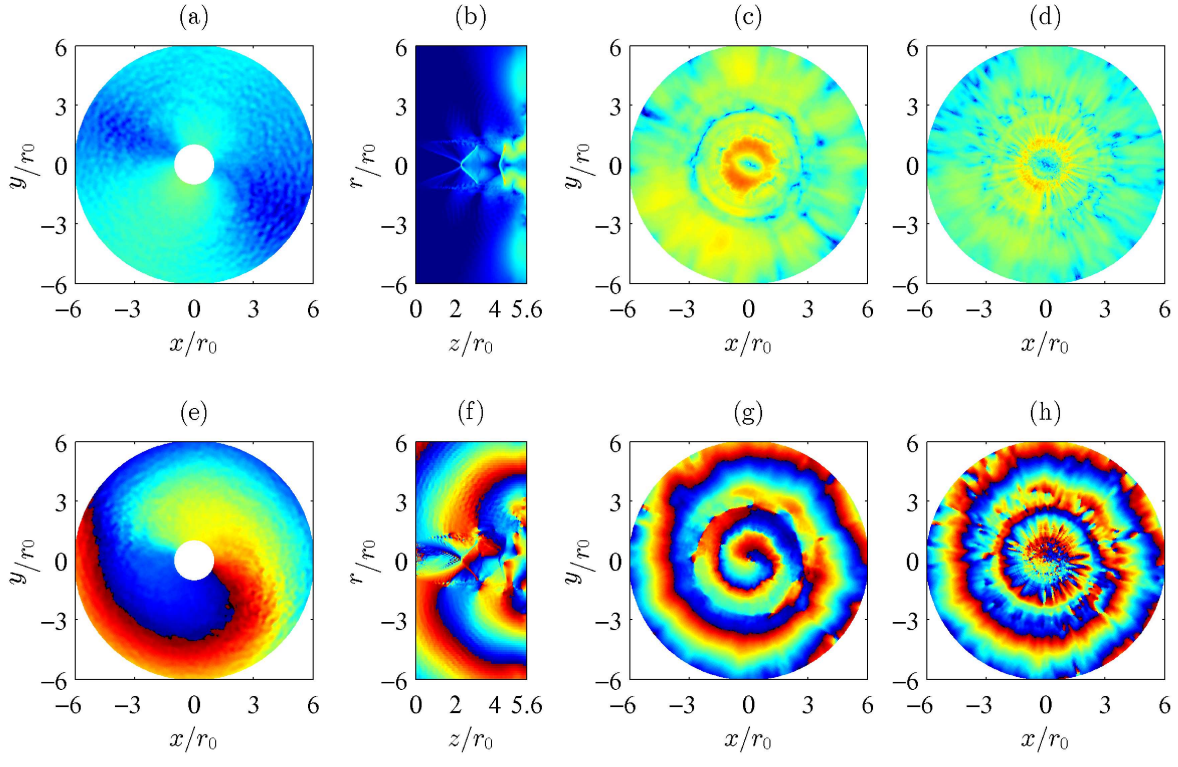

Figure 7. Amplitude (top) and phase (bottom) fields obtained for JetL5 at the dominant tone frequency $St_2 = 0.415$; from pressure (a,e) at $z = 0$, (b,f) at $\theta = 0$ and (c,g) at $z = L$; from density (d,h) at $z = L$.

organized helically in the jet shear layers.

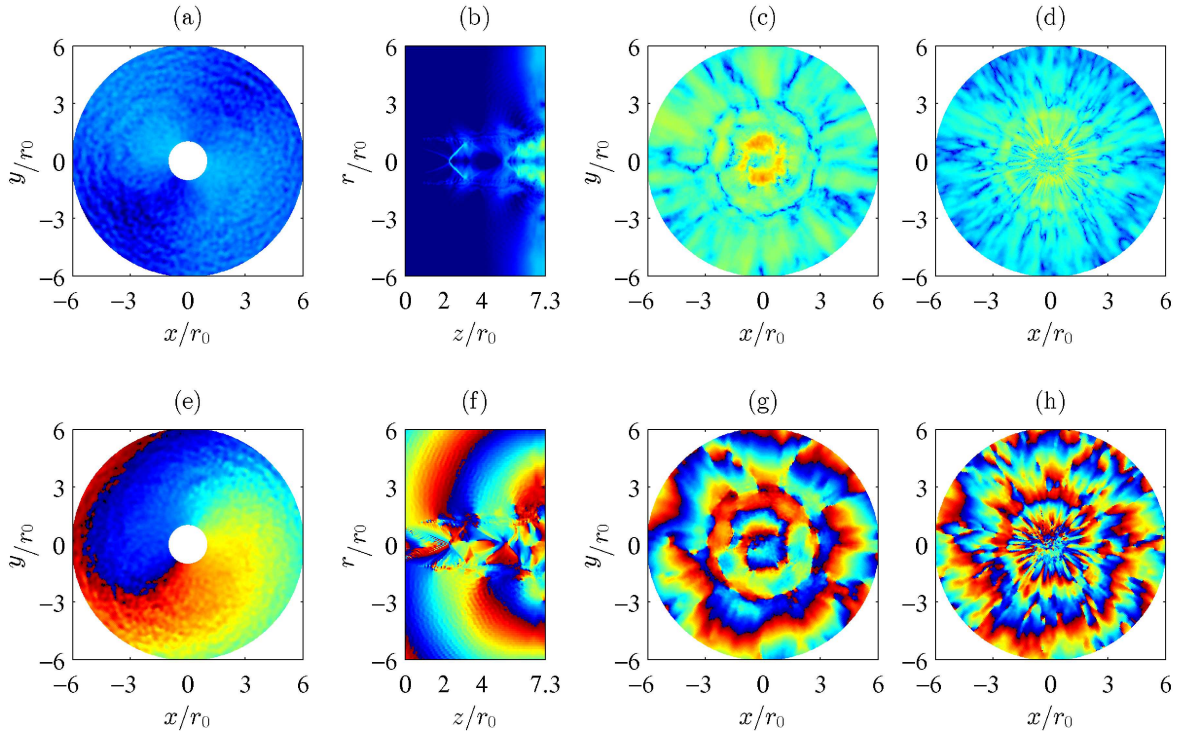

Figure 8. Amplitude (top) and phase (bottom) fields obtained for JetL7 at the dominant tone frequency $St_1 = 0.345$; from pressure (a,e) at $z = 0$, (b,f) at $\theta = 0$ and (c,g) at $z = L$; from density (d,h) at $z = L$.

For JetL9, the amplitude and phase fields for the main tone frequency at $St_2 = 0.34$ are represented in figure 9. Given the phase fields in the planes $z = 0$ and $\theta = 0$ in figures 9(e,f), the tone appears to be associated with an helical oscillation mode of the jet. On the plane $z = L$, spiral shapes are visible in the phase fields, in figures 9(g,h). This indicates a radial propagation on the plate of the turbulent structures organized helically in the jet shear layers.

In order to give further insight into the convection velocity of the structures organised helically in the wall jets for all the jets, the density phase fields on the plate are investigated in the same way as for JetL4 in figure 5. First, let us consider two regions of interest. The first on is near the jet axis over $0 < r < 3r_0$, and the second one is several diameter away over $3r_0 < r < 6r_0$. The mean wavelengths are extracted from the phase fields in each of the two regions. The results for the tone frequencies of JetL4, JetL5 and JetL9 are given in table 4. However, the phase fields of the density fields for the dominant tone frequency of JetL7 at $St_1 = 0.345$ and for the tone frequency of JetL5 at $St_1 = 0.335$ are too noisy, and do not provide converged results. The results found in figure 5 for the dominant tone frequencies of JetL4 at $St_2 = 0.505$ are added.

Jet	St	u_c for $0 < r < 3r_0$	u_c for $3r_0 < r < 6r_0$
JetL4	$St_1 = 0.375$	$u_c = 0.27u_j$	$u_c = 0.40u_j$
JetL4	$St_2 = 0.505$	$u_c = 0.40u_j$	$u_c = 0.49u_j$
JetL5	$St_2 = 0.415$	$u_c = 0.35u_j$	$u_c = 0.47u_j$
JetL9	$St_2 = 0.34$	$u_c = 0.34u_j$	$u_c = 0.46u_j$

Table 4. Mean convection velocities of the turbulent structures in the wall jets for different main tone frequencies.

Over $3r_0 < r < 6r_0$, the convection velocity of the turbulent structures on the wall varies between $0.40u_j$ and $0.49u_j$ for the present jets. Those results are in agreement with the experimental measurements of Davis *et al.*[11] for impinging supersonic ideally expanded round jets. In the phase averaged distributions of the fluctuating pressure, these authors found a convection velocity of the turbulent structures on the wall equals to $0.47u_j$ several diameters away from the jet axis by using Pressure-Sensitive Paint on the flat plate. The results are also consistent with the mean convection velocity found in Gojon *et al.*[12] for the

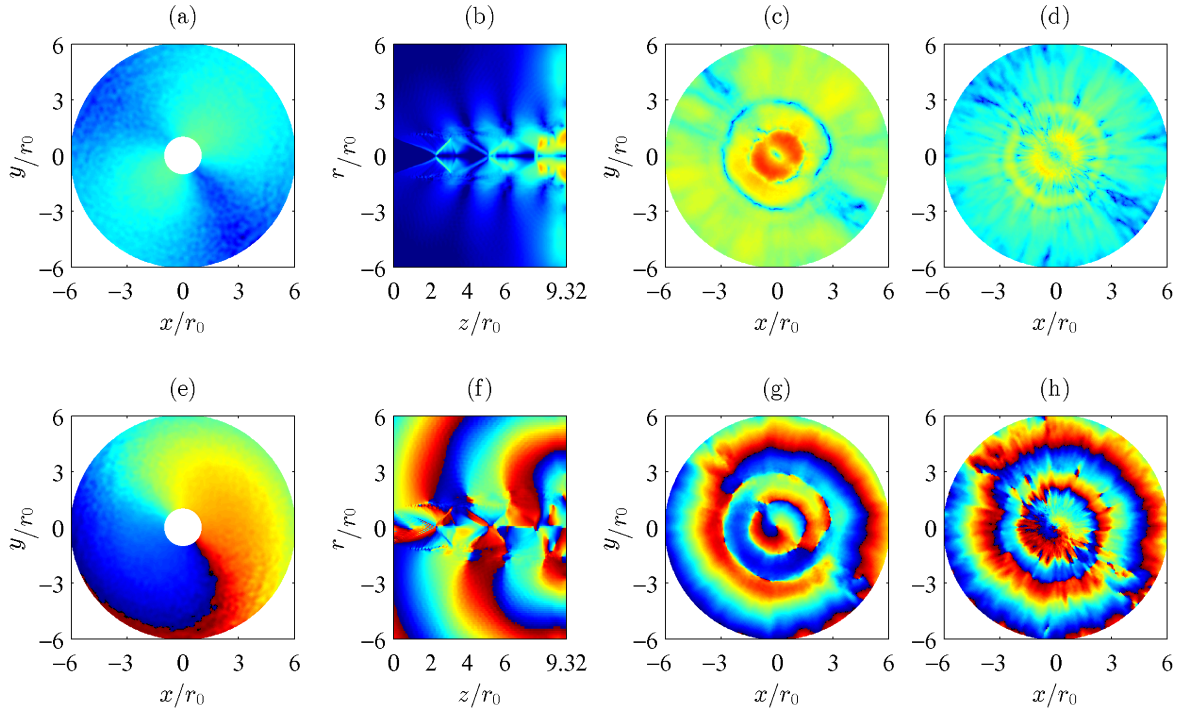

Figure 9. Amplitude (top) and phase (bottom) fields obtained for JetL9 at the dominant tone frequency $St_2 = 0.34$; from pressure (a,e) at $z = 0$, (b,f) at $\theta = 0$ and (c,g) at $z = L$; from density (d,h) at $z = L$.

turbulent structures in the jet shear layer. Indeed, the velocity $< u_c >$ was found to be between $0.54u_j$ and $0.59u_j$ for the present jets. Over $0 < r < 3r_0$, the convection velocity of the turbulent structures on the wall varies between $0.27u_j$ and $0.40u_j$ in the four jets. These values are lower than the value $0.56u_j$ found experimentally by Davis *et al.*[11] in this region of the plate. This difference can be due to the fact that the present jets are non-ideally expanded, leading to the formation of a Mach disk or to the presence of oblique shocks upstream from the plate, see in Gojon *et al.*[12] Thus, the jet shear layers are deviated and impinge on the plate at $r \simeq 2r_0$. Consequently, the mean convection velocities computed near the jet axis do not correspond to the convection velocity of the turbulent structures, as the motion of these structures is not only radial in this region. On the contrary, in an ideally expanded jet, the turbulent structures in the jet shear layers impinge near the jet axis as observed by Krothapalli *et al.*[6] and Davis *et al.*[11] Finally, for JetL4, in the region $3r_0 < r < 6r_0$, the convection velocity of the turbulent structures organised axisymmetrically at the tone frequency $St_2 = 0.505$ is 18% higher than the the convection velocity of the turbulent structures organised helically at $St_1 = 0.375$.

The convection velocity in the wall jets is now computed from radial velocity cross-correlations at one mesh upstream from the plate. The results are represented in figure 10(a) as a function of the radial position between $r = 0$ and $r = 6r_0$. The maximal mean radial velocity in the wall jets is also provided in figure 10(b). In figure 10(a), the mean convection velocity for $r \geq 3r_0$ is of about $0.45u_j$ in the four jets. This result is in good agreement with the convection velocities found from the phase fields for the structures organized axisymmetrically or helically, which are given in table 4. In the region $r \leq 3r_0$, for JetL4, JetL5 and JetL7, a region of negative convection velocity appears around $r = r_0$. In this region, the turbulent structures travel toward the jet axis. This is due to the presence of a recirculation zone near the region of impact, observed experimentally for similar jets by Krothapalli *et al.*[6] This recirculation zone is visible in figure 10(b) with a negative mean radial velocity for $r < r_0$. It is responsible for the difference in the region $0 < r < 3r_0$ between the convection velocities found from the phase fields of the present underexpanded jets and those measured in the phase averaged distributions of the fluctuating pressure of the ideally expanded jets of Davis *et al.*[11]

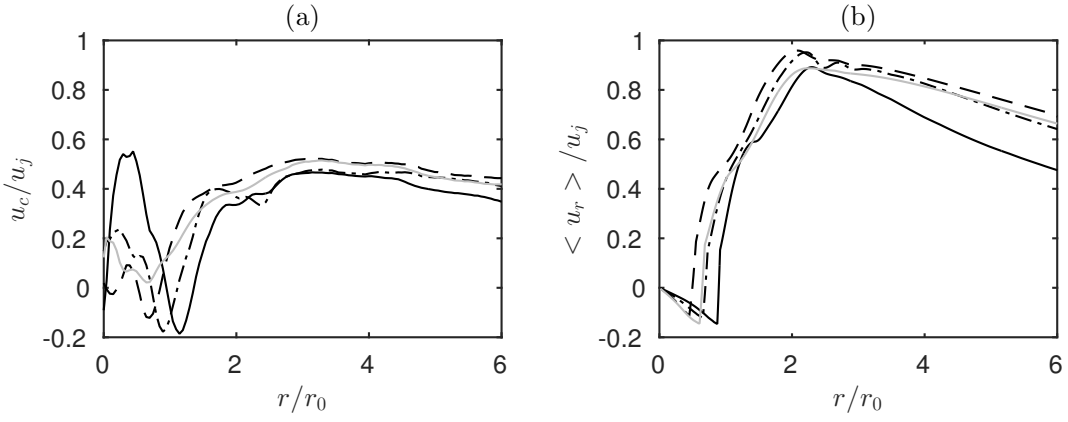

Figure 10. (a) Convection velocity computed from the cross-correlations of radial velocity fluctuations and (b) maximal radial velocity in the wall jet as functions of the radial coordinate for —— JetL4, —·— JetL5, — — — JetL7, and —— JetL9.

IV. Conclusion

In this paper, the azimuthal organisation of the turbulent structures in underexpanded impinging round jets has been studied using compressible large eddy simulation. This organisation is studied in the jet shear-layers but also on the flat plate, in the wall jet created after the impact. The jets are characterized by a Nozzle Pressure Ratio of 4.03, a fully expanded Mach number of 1.56, and a Reynolds number of 6×10^4. The distance between the nozzle and the plate varies from $4.16r_0$ to $9.32r_0$. Shock cell structures and acoustic waves coming from the region of jet impact on the flat plate are observed in the flow snapshots. The spectra in the near pressure fields revealed several tone frequencies due to a feedback mechanism occurring between the nozzle lips and the flat plate. The near pressure and density fields of the jets are then analysed using Fast Fourier Transform on the nozzle exit plane, the plate plane and an azimuthal plane. It has been found found that the helical or axisymmetric organisation of the turbulent structures in the jet shear layers, specific to each tone frequency, persists after the jet impact on the plate. The radial propagation of these structures in the wall jets leads to a spiral shape or to concentric rings in the phase fields, respectively. In particular, for one of the jets, a spiral shape and concentric rings associated with two tone frequencies generated simultaneously have been observed. Finally, the convection velocity of the turbulent structures in the wall jets was evaluated from the phase fields and cross-correlations of radial velocity. Over $3r_0 < r < 6r_0$, the convection velocity of the structures on the wall varies between $0.40u_j$ and $0.49u_j$ in the present jets. These results are in agreement with measurements for ideally expanded impinging supersonic round jets performed using Pressure-Sensitive Paint on the flat plate. Near the jet axis, differences are observed. They are due to the fact that the present jets are non-ideally expanded, leading to the formation of a Mach disk or to the presence of oblique shocks upstream from the plate.

Acknowledgments

This work was performed using HPC resources of P2CHPD (Pôle de Calcul Hautes Performances Dédiés) and IDRIS (Institut du Développement et des Ressources en Informatique Scientifique) under the allocation 2015-2a0204 made by GENCI (Grand Equipement National de Calcul Intensif). This work was performed within the framework of the Labex CeLyA of Université de Lyon, within the program "Investissements d'Avenir" (ANR-10-LABX-0060/ ANR-11-IDEX-0007) operated by the French National Research Agency (ANR).

References

[1] A. Powell. On edge tones and associated phenomena. *Acta Acust. United Ac.*, 3:233–243, 1953.

[2] F.R. Wagner. The sound and flow field of an axially symmetric free jet upon impact on a wall. *NASA*, NASA TT F-13942, 1971.

[3] C.M. Ho and N.S. Nosseir. Dynamics of an impinging jet. part 1. The feedback phenomenon. *J. Fluid Mech.*, 105:119–142, 1981.

[4] N.S. Nosseir and C.M. Ho. Dynamics of an impinging jet. part 2. The noise generation. *J. Fluid Mech.*, 116:379–391, 1982.

[5] B. Henderson and A. Powell. Experiments concerning tones produced by an axisymmetric choked jet impinging on flat plates. *J. Sound Vib.*, 168(2):307–326, 1993.

[6] A. Krothapalli, E. Rajkuperan, F. Alvi, and L. Lourenco. Flow field and noise characteristics of a supersonic impinging jet. *J. Fluid Mech.*, 392:155–181, 1999.

[7] B. Henderson, J. Bridges, and M. Wernet. An experimental study of the oscillatory flow structure of tone-producing supersonic impinging jets. *J. Fluid Mech.*, 542:115–137, 2005.

[8] A. Risborg and J. Soria. High-speed optical measurements of an underexpanded supersonic jet impinging on an inclined plate. *28th International Congress on High-Speed Imaging and Photonics*, 7126(F), 2009.

[9] N.A. Buchmann, D.M. Mitchell, K.M. Ingvorsen, D.R. Honnery, and J. Soria. High spatial resolution imaging of a supersonic underexpanded jet impinging on a flat plate. *6th Australian Conference on Laser Diagnostics in Fluid Mechanics and Combustion*, 2011.

[10] D.M. Mitchell, D.R. Honnery, and J. Soria. The visualization of the acoustic feedback loop in impinging underexpanded supersonic jet flows using ultra-high frame rate schlieren. *J. of visualization*, 15(4):333–341, 2012.

[11] T. Davis, A. Edstrand, F. Alvi, L. Cattafesta, D. Yorita, and K. Asai. Investigation of impinging jet resonant modes using unsteady pressure-sensitive paint measurements. *Exp. in Fluids*, 56(5):1–13, 2015.

[12] R. Gojon, C. Bogey, and O. Marsden. Large-eddy simulation of underexpanded round jets impinging on a flat plate 4 to 9 radii downstream from the nozzle. *AIAA Paper 2015-2210*, 2015.

[13] C. Bogey and C. Bailly. A family of low dispersive and low dissipative explicit schemes for flow and noise computations. *J. Comput. Phys.*, 194(1):194–214, 2004.

[14] J. Berland, C. Bogey, O. Marsden, and C. Bailly. High-order, low dispersive and low dissipative explicit schemes for multiple-scale and boundary problems. *J. Comput. Phys.*, 224(2):637–662, 2007.

[15] C. Bogey and C. Bailly. Large eddy simulations of transitional round jets: influence of the Reynolds number on flow development and energy dissipation. *Phys. Fluids*, 18:065101, 2006.

[16] C. Bogey and C. Bailly. Turbulence and energy budget in a self-preserving round jet: direct evaluation using large eddy simulation. *J. Fluid Mech.*, 627:129–160, 2009.

[17] C.K.W. Tam and Z. Dong. Wall boundary conditions for high-order finite-difference schemes in computational aeroacoustics. *Theor. Comput. Fluid Dyn*, 6:303–322, 1994.

[18] C. Bogey, N. de Cacqueray, and C. Bailly. A shock-capturing methodology based on adaptative spatial filtering for high-order non-linear computations. *J. Comput. Phys.*, 228(5):1447–1465, 2009.

[19] K. Mohseni and T. Colonius. Numerical treatment of polar coordinate singularities. *J. Comput. Phys.*, 157(2):787–795, 2000.

[20] C. Bogey, N. de Cacqueray, and C. Bailly. Finite differences for coarse azimuthal discretization and for reduction of effective resolution near origin of cylindrical flow equations. *J. Comput. Phys.*, 230(4): 1134–1146, 2011.

[21] C. Bogey, O. Marsden, and C. Bailly. Large-eddy simulation of the flow and acoustic fields of a Reynolds number 10^5 subsonic jet with tripped exit boundary layers. *Phys. Fluids*, 23:035104, 2011.

[22] R. Gojon, C. Bogey, and O. Marsden. Large-eddy simulation of supersonic planar jets impinging on a flat plate at an angle of 60 to 90 degrees. *AIAA Paper 2015-2209*, 2015.